International Journal of Composite Materials 2017, 7(5): 144-149
DOI: 10.5923/j.cmaterials.20170705.03

Evaluation of in Vitro Bioactivity of 45S5 Bioactive Glass/Poly Lactic Acid Scaffolds Produced by 3D Printing

Santos Adriana Martel Estrada[1], Imelda Olivas Armendáriz[2,*], Alecia Torres García[2], Juan Francisco Hernández Paz[2], Claudia Alejandra Rodríguez González[2]

[1]Departamento de Diseño, Universidad Autónoma de Ciudad Juárez, Ciudad Juárez, México
[2]Departmento de Ciencias Básicas, Universidad Autónoma de Ciudad Juárez, Ciudad Juárez, México

Abstract In this study 45S5 Bioactive Glass-based scaffolds produced by 3D Printing techniques have been evaluated. Three-dimensional printing (3DP) technique was used to fabricate scaffolds with a novel micro- and macro-architecture. In this study, Poly Lactic Acid/45S5 bioactive glass composites were produced. 45S5 bioactive glass was synthetized by sol-gel process using microwave exposure. Cylindrical scaffolds of different designs were fabricated. The in vitro bioactivity of the composites was investigated by incubation in simulated body fluid (SBF). The apatite layer was assessed using scanning electronic microscope (SEM) coupled to energy-dispersive electron X-ray spectroscopy and confirmed using X-ray diffraction (XRD) and Fourier-Transformed Infrared spectroscopy (FTIR). Results confirmed that after incubation in simulated body fluid, it was formed a layer of carbonate hydroxyapatite in the surface of the scaffolds.

Keywords 45S5 Bioactive glass, Poly lactic acid, 3D printing

1. Introduction

In recent years, as an alternative to limitations of current grafting procedures, bone tissue engineering has emerged as a different strategy which provides a solution to regenerate or repair bone tissue [1]. Researchers have taken into account three elements such as osteoinductive growth factors, osteogenic progenitor cells, and osteoconductive biomaterials. The performance of biomaterials (3D scaffold) depends of the success of the material in these aspects (bone tissue engineering). Since these artificial structures act as temporary extracellular matrix, which must allow the adhesion, migration, and proliferation of cells as well as maintain cellular differentiation. In addition, the scaffold must be fabricated with defined morphology (interconnected structure and controlled porosity) as well as suitable mechanical properties [2]. For this reason, it has been used different techniques and multi-phase materials with structure and composition similar to natural bone during the fabrication of the structure.

The ability of apatite to form on the surface of a material, is often evaluated in a simulated body fluid [3]. Bioactivity refers to a spontaneous interaction of material with the surrounding biological environment that induce precipitation and mineralization of calcium phosphates on the surface, that it is affected by the physical and chemical properties of it [4]. After the scaffold is implanted into bone defect, it is expected that it well integrate with the surrounding bone without forming fibrous tissue interface layer [5].

Some studies have shown that bioactivity glasses bond with bone more rapidly than other bioceramics [6]. Hydroxyapatite, tri-calcium phosphate (TCP) and bioactive glass have been used widely in biomaterials to interact with tissues and promote osteogenesis. However, the brittle nature of commercial bioactive materials made of HA, results in low mechanical attributes [7].

The most common commercial bioactive glass is the 45S5. It is composed of SiO_2, Na_2O, CaO and P_2O_5. It contains less than 60% of SiO_2, high contents of Na_2O and CaO, and a CaO/P_2O_5 high ratio that make this material bioactive and very reactive in aqueous medias. Bioactive glasses can be synthetized by melting and casting or by sol-gel methods [8-10]. Melting temperatures are above 1100-1300℃. Lower synthesis temperatures, more homogeneous composition and high surface area are the main advantages of sol-gel over the melting and casting process [8, 10-12]. However, the sol-gel technique for synthetizing 45S5 bioactive glass requires several steps that includes: sol and gel forming, aging (usually 24 h at 70℃), drying (Approximately 24 h at 120℃) and a last step for stabilizing and removing the remaining nitrates of the resulting material which is usually performed at approximately 24 h at 700℃. During this last process, crystallization can occurs reducing the glass bioactivity [13]. Microwave processing is another synthesis methodology. It provides a faster, volumetric and more selective heating that

* Corresponding author:
iolivas@@uacj.mx (Imelda Olivas Armendáriz)
Published online at http://journal.sapub.org/cmaterials

results in a reduction of the processing time, energy savings and dimensional stability. Many materials do not absorb the microwaves at low temperatures and therefore additional heating elements are required in the initial stages [14, 15]. In the case of the glasses, it has been reported that they must reach a critic temperature to absorb microwaves [16]. Thus, microwave heating for glass processing is generally used only in some steps of the process (e.g. drying) or using additional heating elements [14, 17].

Polylactic acid (PLA) is a linear aliphatic polyesters, which is most used in bone tissue engineering for its mechanical integrity is preserved in vitro or in vivo In addition to being one of the polymers accepted by the Food and Drug Administration (FDA). For being a biodegradable and biocompatible polymer, it has been used in medical applications including tissue engineering [2], surgical suture [18], drug release systems [19], biomedical imaging and detection, solubilization of hydrophobic drugs and bioactive agents [20], dental implant coating [21], fracture fixation [22], among others.

Several methods have been used to elaborate scaffolds for tissue engineering such as electrospinning [23], foaming [24], atmospheric pressure plasma assisted modification [25], three dimensional printing [26], supercritical carbon dioxide foaming [27], particle leaching technique [28], freeze drying [29] and so on.

3D printing allows the production of porous scaffold with complex geometries containing internal pore architectures that are reproduced using a computer generated model [30]. Through this method it is possible to produce macropores designed to allow the ingrowth of host tissues [31]. There are more than 40 differents 3D-printing techniques in development, including fused deposition modeling, stereolithography, inkjet printing, selective laser sintering and color jet printing [32].

SBF immersion study is an effective method to evaluate bioactivity by degradation mechanism (weight loss analysis), apatite formation on material surface and calcium to phosphorus ratio (Ca:P) [7].

2. Methods

Bioactive glass 45S5 was synthetized by sol-gel process (45% SiO_2, 24.5% Na_2O, 24.5% CaO and 6% P_2O_5 in molar percentage). Initially, a 1M solution of nitric acid was prepared with H_2O, then 33.5 ml of Si $(OC_2H_5)_4$ (TEOS, alpha Aesar tetraethyl orthosilicate) were added and the mixture was stirred during 60 min to promote hydrolysis. Subsequently, 2.9 ml of $(C_2H_5O)_3PO$ (TEP, Alfa Aesar tetraethyl phosphate), 20.13 g $Ca(NO)_3$ (Alpha Aesar calcium nitrate), 4 ml H_2O, and 13.52 g $NaNO_3$ (Alpha Aesar sodium nitrate) were added and stirred during 45 minutes until a clear sol was obtained. The sol was stored in a closed container during 5 days at room temperature to form the gel. Then, the resulting gel was aged in the closed container for 1 day at 70℃ and dried at 120℃ during 1 day.

Finally, for dry gel stabilization, one gram of the dry gel was placed on a mullite crucible isolated with high alumina fiber and exposed to microwave radiation in a conventional household microwave (Emerson, MT3070 model, 120V-60Hz power supply, 2450MHz frequency, 1100 Watts power) during 1.5 to 6 minutes and then quenched in air. Translucid glass was obtained and characterized by a Panalytical X'Pert PRO powder X-Ray diffraction instrument with Cu Kα radiation (λ = 0.15418 nm) at 40 kV and 20 mA, a Fourier-transformed infrared spectrophotometer (Nicolet 6700 FT-IR Thermo Scientific) and a Broker Energy Dispersive X-Ray Spectroscope. For comparative purposes, dry gel samples were also stabilized in a conventional furnace at 700℃ during 24 h.

PLA/45S5 bioactive glass was fabricated by mechanical mixing. Firstly, PLA powders were obtained using a mill to grind the polymer pellets, Then, PLA were mixed with 45S5 bioactive glass powders mechanically. After this procedure, the mixed was put on an extruder (ExtrusionBot™) to get a filament.

For the bioactivity test it was used a sample (1 cm x 1 cm x 0.5 cm) of PLA and PLA/45S5 bioactive glass that was printed previously in a MakerBoot 3D printer using 75 % of filler as a parameter. A previously established method for this test was used [Martel-Estrada, 2011]. Briefly, the samples were immersed in 5 mL of the SBF (pH 7.4) at 37◦C. At each time point, the samples were removed from the SBF, rinsed with de-ionized water, and dried at room temperature.

After immersion the samples into the SBF for the different periods, the surface morphologies of the deposits were observed using a field emission scanning electron microscopy (Jeol JSM-7000F). The compositions of the deposits were analyzed using an X-ray diffractometer (X Pret PRO PANalytical) and a Fourier-transformed infrared spectrophotometer (Nicolet 6700 FT-IR Thermo Scientific).

3. Results and Discussion

3D printing has been employed to fabricate scaffolds for bone engineering to stimulate bone regeneration and combat infection [33]. Poly(L-lactic acid) has been studied for use in biomedical applications such as sutures, scaffolds for tissue engineering, orthopedic devices, or drug delivery systems due to its biocompatibility and bioresorbability [34]. On the other hand, bioactive glass has attracted attention due to its excellent biocompatibility and bioactivity [35]. So, during this research, the bioactivity properties of PLA/45S5 Bioglass composite produced by 3D printing procedure was evaluated.

The bioactive glass stabilized by microwave is shown in Figure 1. It was found that the dry gel absorbed the microwaves and no additional heating source is needed.

Figure 1. Visual appearance of the bioactive glass 45S5 synthetized by sol gel method using microwave for dry gel stabilization. 1.5 and 3 minutes exposure were not enough to melt the sample and obtain translucid glass

Figure 2 shows that exposing the dry gel to microwaves for 6 minutes is sufficient to achieve an amorphous bioactive glass. Nitrates presence ($NaNO_3$) disappear after 3 minutes exposure and some crystalline phases start appearing with time ($Na_6Ca_3Si_6O_{18}$) (PDF 01-077-2189), Na_4Ca_4 (Si_6O_{18}) (PDF 01-075-1687, 01- 079-1084, 01-0791086, 01-079-1087, 01-079-1089 and 01-078-0364), Na4.2Ca2.8 (Si_6O_{18}) (PDF 01-078-1649) and Ca (Si_2O_5) (PDF 01-089-6267). Li et al. [11] reported same phases for 45S5 bioactive glass stabilized at 700℃ during 24 h. In some cases, presence of crystalline phases containing calcium and phosphorous appear. For example, in 2010 Pirayesh et al. [13] reported the presence of the Na_2Ca_4 (PO_4) SiO_4 phase under the same conditions of stabilization. Crystalline phases containing phosphorous and calcium are not desirable since these phases are reported to be inert and therefore, they reduce the material's bioactivity. After 6 minutes of microwave exposure, the mixture melts and after air quenching an amorphous material is formed.

EDS spectra (Figure 3) show the elements forming the bioactive glass after 6 minutes to microwave exposure. Presence of the typical elements of the 45S5 composition are observed which include Calcium (Ca), Silicon (Si), Phosphorous (P), Sodium (Na) and Oxygen.

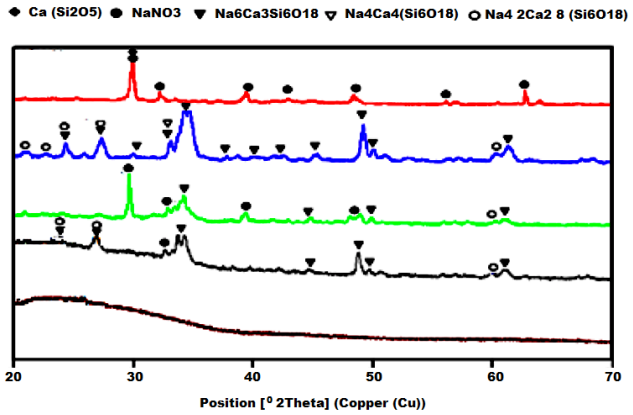

Figure 2. XRD analysis of dry gel after different time microwave exposure. Red color diffractogram is for dry gel before stabilization, blue for dry gel after stabilization in conventional furnace (700℃, 24 h), green for dry gel after stabilization (1.5 min, microwave), black for dry gel after stabilization (3 min, microwave), brown for dry gel after stabilization-translucid glass (6 min, microwave)

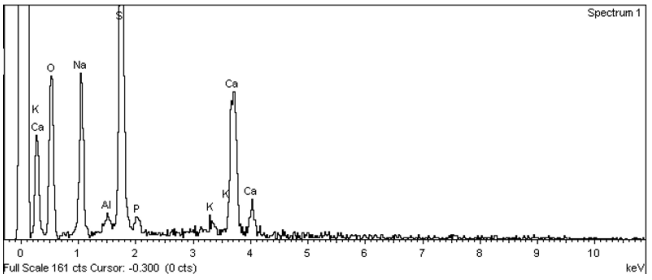

Figure 3. EDS analysis of the bioactive glass 45S5

Figure 4 shows the FTIR analysis of the bioactive glass exposed to microwave after 6 minutes and quenched in air and the bioactive glass stabilized in conventional oven at 700℃ during 24 h. Main difference is that the bioactive glass obtained using microwave does not exhibit functional groups at 578 cm^{-1} and 620 cm^{-1} wavelengths which correspond to the P-O binding of crystalline phases [13, 36, 37].

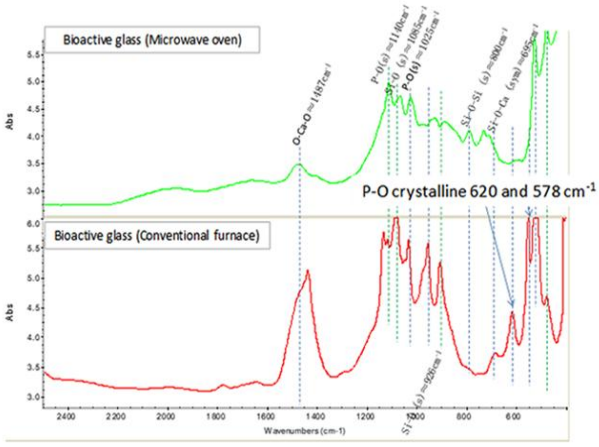

Figure 4. FTIR analysis comparison of bioactive glass stabilized in conventional oven (700℃, 24 h), and using microwave

3D printing is an inexpensive way to manufacture scaffolding for tissue engineering. The cost of the equipment

represents an investment around 3000 dollars. Also the manufacturing time is reduced from approximately 36 hours by lyophilization to only minutes using this procedure. For this experiment, it was design a simple rectangular prism of 1 cm x 1 cm x 0.5 cm using a CAD program. Then, to get the scaffold it was used a 75% of filler as a parameter for the printer. This scaffold was used as a sample for the bioactivity test.

There are several methods to evaluate the bioactivity of a material. The most used is the *in vitro* test that involves a material that accelerates the heterogeneous crystallization of apatite in a supersaturated solution towards hydroxyapatite [38]. This ability of the material is an important indication of their osteointegration capability and bioactivity. This can be done in several ways including a local change of supersaturation thus promoting apatite precipitation [39]. On the other hand, it has been reported that PLA and bioactive glass once exposed to SBF cause a change in the local pH resulting in an acceleration of apatite nucleation. Figure 5 shows the SEM images of scaffolds, before and after being exposed to SBF for 1, 3, and 7 days. The figures 5a) and 5b) show a porous and interconnected structure in both supports however the surface on PLA scaffold is smoother than the PLA scaffold with the bioactive glass where particles can be observed. On the other hand, after 1 day of immersion it can be observed the deposition of a few newly apatite spherical clusters on the surface of the PLA scaffold (Fig. 5 c)) meanwhile the PLA/BG scaffold shows a whole covered surface with a great amount of deposited crystals (Fig. 5 d). After 3 days, the deposition of crystals increased in thickness with a structure of cauliflower like in the PLA/BG scaffold (Fig. 5 e), continuing with the same tendency of the first day since the crystals almost completely cover the surface scaffold and on the PLA support is incomplete (Fig. 5 f). Furthermore it can be seen, in the PLA/BG, how the pores are already being filled by the deposited apatite. At 7 days of immersion, the deposition of aggregates of apatite-like crystals continues to increase in both scaffolds (Fig. 5g) and 5h) however in the PLA/BG support the surface has been completely covered most of pores.

These results can be assigned to the change of the local pH which increase the local supersaturation of calcium and phosphate ions for the weak acidic COOH group generated during the partially hydrolyzed of PLA, whereby a negatively charged polymeric surface and can be bind to Ca^{2+} through hydrogen bonding and electrostatic force [40] and the ionic exchange between the fluid (H+ o H_3O+). XRD analyses of Figure 6 and 7 evidence this, where the biological apatite phase is being detected despite the short time of exposure.

In the case of the PLA/BG scaffolds the ionic exchange increases due to the dissolution of the glass network. Migration of Ca_2+ and PO_4^{3-} ions change the pH of the solution enhancing the biological apatite formation. XRD analysis of PLA/BG (Figure 7) shows the apatite presence as well as an increment of the reflection intensity of the peak at 22^o 2Θ angle which could correspond to some crystallization of the SiO_2 of the dissolved glass. (SiO_2 main diffraction peak is at 22^o 2Θ angle).

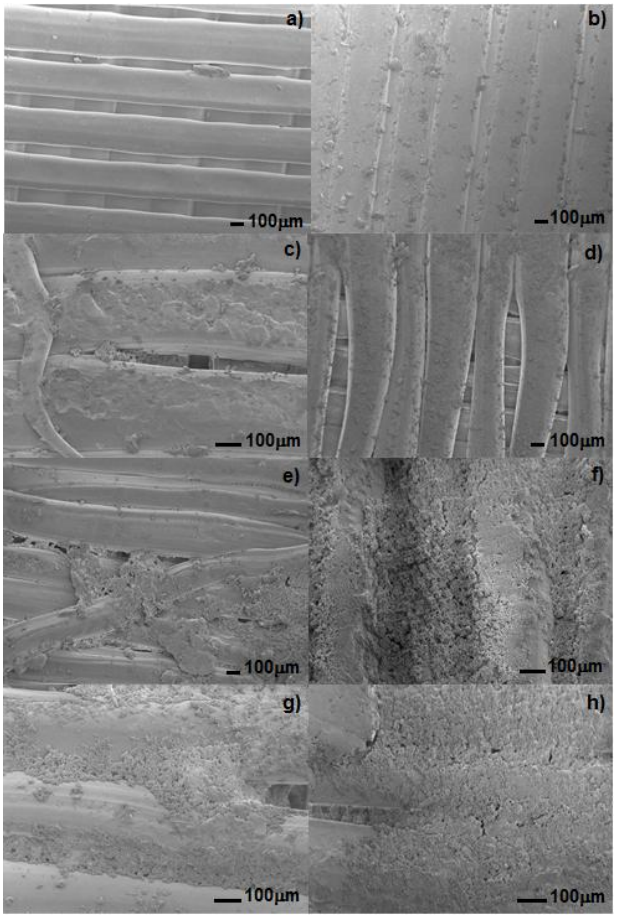

Figure 5. The SEM images of the materials before and after being exposed to SBF for 1, 3, and 7 days. (a) PLA and (b) PLA/BG before being exposed to SBF. The SEM images of the materials mineral deposition of PLA and PLA/BG scaffolds after 1, 3, and 7 days in SBF. (c) PLA scaffolds at 1 day, (e) PLA scaffolds at 3 days, (g) PLA scaffolds at 7 days, (d) PLA/BG at 1 day, (f) PLA/BG at 3 days, and (h) PLA/BG at 7 days

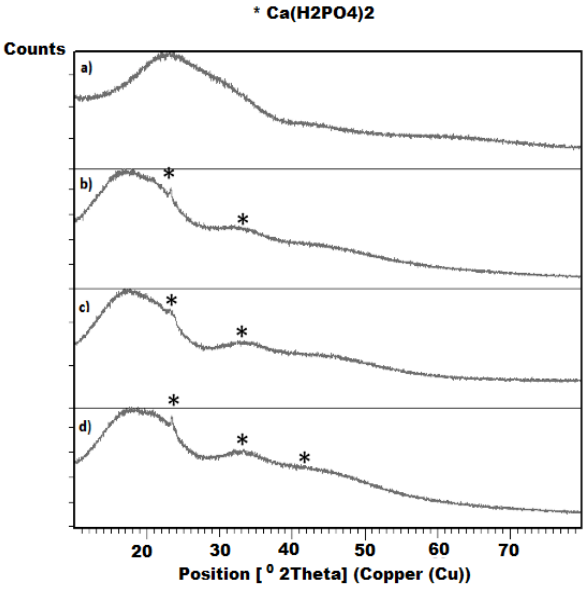

Figure 6. XRD analysis of PLA scaffolds exposed to the bioactivity test

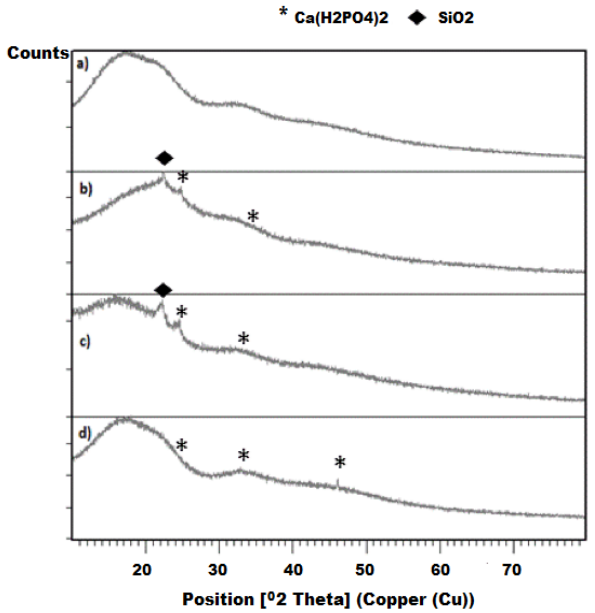

Figure 7. XRD analysis of PLA/BG scaffolds exposed to the bioactivity test

Finally, Figure 8 shows the infrared spectra for the various samples after the SBF treatment. It is possible to see the presence of the bands assigned to the phosphate bending vibration at 1079, 670, 609 and 570 cm^{-1} and carbonate group out of plane and stretching mode at 858 and 1451 cm^{-1}. It is evidence that suggest that carbonated apatite was formed and more intense in the PLA/BG composite than in PLA.

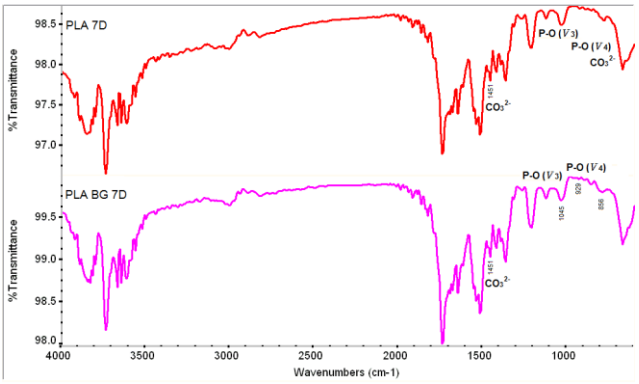

Figure 8. FTIR spectra for the samples after the SBF treatment

4. Conclusions

Bioactive glass 45S5 was successfully synthetized by sol-gel process using microwave for removing nitrates phases from dry gels. The microwave processing allow to reduce the stabilization time (24 h to 7 minutes for X g) and no crystallization occurred maintaining the desired bioactivity. The composition and parameters of printing were selected considering the design of scaffolds with suitable chemical, mechanical and morphological properties for their use in bone regeneration.

REFERENCES

[1] Atak BH, Buyuk B, Huysal M, Isik S, Senel M, Metzger W, et al. Preparation and characterization of amine functional nano-hydroxyapatite/chitosan bionanocomposite for bone tissue engineering applications. Carbohydr Polym. 2017; 164: 200-213.

[2] Kurtycz P, Ciach T, Olszyna A, Kunicki A, Radziun E, Roslon M, et al. Electrospun poly(L-lactic)acid/nanoalumina (PLA/Al_2O_3) composite fiber mats with potential biomedical application — Investigation of cytotoxicity. Fibers and Polymers. 2013; 14(4): 578-583.

[3] Kokubo T, Takadama H. How useful is SBF in predicting in vivo bone bioactivity? Biomaterials. 2006; 27(15): 2907-2915.

[4] Zhang J, Dai C, Wei J, Wen Z, Zhang S, Chen C. Degradable behavior and bioactivity of micro-arc oxidized AZ91D Mg alloy with calcium phosphate/chitosan composite coating in m-SBF. Colloids and Surfaces B: Biointerfaces. 2013; 111: 179-187.

[5] Huang L, Zhou B, Wu H, Zheng L, Zhao J. Effect of apatite formation of biphasic calcium phosphate ceramic (BCP) on osteoblastogenesis using simulated body fluid (SBF) with or without bovine serum albumin (BSA). Materials Science and Engineering: C. 2017; 70, Part 2:955-961.

[6] Jmal N, Bouaziz J. Synthesis, characterization and bioactivity of a calcium-phosphate glass-ceramics obtained by the sol-gel processing method. Materials science & engineering C, Materials for biological applications. 2017; 71: 279-288.

[7] Shahabudin NS, Ahmad ZA, Abdullah NS. Alumina Foam (AF) Fabrication Optimization and SBF Immersion Studies for AF, Hydroxyapatite (HA) Coated AF (HACAF) and HA-bentonite Coated AF (HABCAF) Bone Tissue Scaffolds. Procedia Chemistry. 2016; 19: 884-890.

[8] Hench LL. Chronology of Bioactive Glass Development and Clinical Applications. New Journal of Glass and Ceramics. 2013; 3: 67-73.

[9] Rahaman MN, Day DE, Bal BS, Fu Q, Jung SB, Bonewald LF, et al. Bioactive glass in tissue engineering. Acta biomaterialia. 2011;7(6): 2355-2373.

[10] Sepulveda P, Jones JR, Hench LL. Characterization of melt-derived 45S5 and sol-gel–derived 58S bioactive glasses. Journal of Biomedical Materials Research. 2001; 58(6): 734-740.

[11] Li R, Clark AE, Hench LL. An investigation of bioactive glass powders by sol-gel processing. Journal of Applied Biomaterials. 1991; 2(4): 231-239.

[12] Polini A, Bai H, Tomsia AP. Dental applications of nanostructured bioactive glass and its composites. Wiley Interdiscip Rev Nanomed Nanobiotechnol. 2013; 5(4): 399-410.

[13] Pirayesh H. Effects manufacturing method on surface mineralization of bioactive glasses. 2010.

[14] Jamuna-Thevi K, Zakaria FA, Othman R, Muhamad S. Development of macroporous calcium phosphate scaffold processed via microwave rapid drying. Materials Science and Engineering: C. 2009; 29(5): 1732-1740.

[15] Clark DE, Sutton WH. Microwave processing of materials. Annual Review of Materials Science. 1996; 26(1): 299-331.

[16] Buchanan LA, El-Ghannam A. Effect of bioactive glass crystallization on the conformation and bioactivity of adsorbed proteins. Journal of biomedical materials research Part A. 2010; 93(2): 537-546.

[17] Wang X, Fan H, Xiao Y, Zhang X. Fabrication and characterization of porous hydroxyapatite/β-tricalcium phosphate ceramics by microwave sintering. Materials Letters. 2006; 60(4): 455-458.

[18] Kim KI, Kim WK, Seo DK, Yoo IS, Kim EK, Yoon HH. Production of lactic acid from food wastes. Applied biochemistry and biotechnology. 2003; 107(1): 637-647.

[19] Luo Y-L, Huang R-J, Xu F, Chen Y-S. pH-Sensitive biodegradable PMAA2-b-PLA-b-PMAA2 H-type multiblock copolymer micelles: synthesis, characterization, and drug release applications. Journal of Materials Science. 2014; 49(22): 7730-7741.

[20] Lee Y-K, Hong SM, Kim JS, Im JH, Min HS, Subramanyam E, et al. Encapsulation of CdSe/ZnS quantum dots in poly(ethylene glycol)-poly(D,L-lactide) micelle for biomedical imaging and detection. Macromolecular Research. 2007; 15(4): 330-336.

[21] Shahi RG, Albuquerque MTP, Munchow EA, Blanchard SB, Gregory RL, Bottino MC. Novel bioactive tetracycline-containing electrospun polymer fibers as a potential antibacterial dental implant coating. Odontology. 2017; 105(3): 354-363.

[22] Heidari BS, Oliaei E, Shayesteh H, Davachi SM, Hejazi I, Seyfi J, et al. Simulation of mechanical behavior and optimization of simulated injection molding process for PLA based antibacterial composite and nanocomposite bone screws using central composite design. Journal of the mechanical behavior of biomedical materials. 2017; 65: 160-176.

[23] Aldana AA, Abraham GA. Current advances in electrospun gelatin-based scaffolds for tissue engineering applications. International journal of pharmaceutics. 2017; 523(2): 441-453.

[24] Caroline C, Raya B, Daniel C, Benjamin D, Christophe T, Philippe B, et al. Elaboration and evaluation of alginate foam scaffolds for soft tissue engineering. International journal of pharmaceutics. 2017; 524(1–2): 433-442.

[25] Kudryavtseva V, Stankevich K, Gudima A, Kibler E, Zhukov Y, Bolbasov E, et al. Atmospheric pressure plasma assisted immobilization of hyaluronic acid on tissue engineering PLA-based scaffolds and its effect on primary human macrophages. Materials & Design.

[26] Zhao H, Liang W. A novel comby scaffold with improved mechanical strength for bone tissue engineering. Materials Letters. 2017; 194: 220-223.

[27] Kuang T, Chen F, Chang L, Zhao Y, Fu D, Gong X, et al. Facile preparation of open-cellular porous poly (l-lactic acid) scaffold by supercritical carbon dioxide foaming for potential tissue engineering applications. Chemical Engineering Journal. 2017; 307: 1017-1025.

[28] Wang Y, Qian J, Zhao N, Liu T, Xu W, Suo A. Novel hydroxyethyl chitosan/cellulose scaffolds with bubble-like porous structure for bone tissue engineering. Carbohydrate Polymers. 2017; 167: 44-51.

[29] Abd-Khorsand S, Saber-Samandari S, Saber-Samandari S. Development of nanocomposite scaffolds based on TiO2 doped in grafted chitosan/hydroxyapatite by freeze drying method and evaluation of biocompatibility. International journal of biological macromolecules. 2017; 101: 51-58.

[30] Bracaglia LG, Smith BT, Watson E, Arumugasaamy N, Mikos AG, Fisher JP. 3D printing for the design and fabrication of polymer-based gradient scaffolds. Acta biomaterialia.

[31] Zhang W, Feng C, Yang G, Li G, Ding X, Wang S, et al. 3D-printed scaffolds with synergistic effect of hollow-pipe structure and bioactive ions for vascularized bone regeneration. Biomaterials. 2017; 135: 85-95.

[32] Wang X, Jiang M, Zhou Z, Gou J, Hui D. 3D printing of polymer matrix composites: A review and prospective. Composites Part B: Engineering. 2017; 110: 442-458.

[33] Inzana J, Olvera, D., Fuller, S., Kelly, J., Graeve, O., Schwarz, E., Kates, S., Awad, H. 3D printing of composite calcium phosphate and collagen scaffolds for bone regeneration. Biomaterials. 2014; 35: 4026-4034.

[34] Tanase C, Spiridon, I. PLA/chitosan/keratin composites for biomedical applications. Materials science & engineering C. 2014: 242-247.

[35] Xin R, Zhang, Q., Gao, J. Identification of wollastonite phase in sintered 45S5 bioglass and its effect on in vitro bioactivity. Journal of Non-Crystalline Solids. 2010;365:1180-1184.

[36] Li X, Wang L, Fan Y, Feng Q, Cui FZ, Watari F. Nanostructured scaffolds for bone tissue engineering. Journal of biomedical materials research Part A. 2013; 101(8): 2424-2435.

[37] Saiz E, Gremillard L, Menendez G, Miranda P, Gryn K, Tomsia AP. Preparation of porous hydroxyapatite scaffolds. Materials Science and Engineering: C. 2007; 27(3): 546-550.

[38] Kokubo T, Takadama H. How useful is SBF in predicting in vivo bone bioactivity? Biomaterials. 2006; 27(15): 2907-2915.

[39] Bohner M, Lemaitre J. Can bioactivity be tested in vitro with SBF solution? Biomaterials. 2009; 30(12): 2175-2179.

[40] Zhang R, Ma PX. Porous poly(L-lactic acid)/apatite composites created by biomimetic process. Journal of Biomedical Materials Research. 1999; 45(4): 285-293.